

# Effects of Pb doping on structural and electronic properties of $\text{Bi}_2\text{Sr}_2\text{Ca}_2\text{Cu}_3\text{O}_{10}$



J.A. Camargo-Martínez<sup>a,\*</sup>, R. Baquero<sup>b</sup>

<sup>a</sup>Grupo de Investigación en Ciencias Básicas, Aplicación e Innovación – CIBAIN, Fundación Universitaria Internacional del Trópico Americano – Unitrópico, Yopal, Colombia

<sup>b</sup>Departamento de Física, CINVESTAV-IPN, Av. IPN 2508, México 07360, Mexico

## ARTICLE INFO

### Article history:

Received 21 September 2015

Revised 30 November 2015

Accepted 21 December 2015

Available online 30 December 2015

### Keywords:

Bi2223

Electronic structure

Band structure

Fermi surface

Virtual crystal approximation

Pb-doped

## ABSTRACT

Pb doping effect in the  $\text{Bi}_2\text{Sr}_2\text{Ca}_2\text{Cu}_3\text{O}_{10}$  compound (Bi2223) on the structural and electronic properties were investigated, using the Local Density (LDA) and Virtual Crystal (VCA) approximations within the framework of the Density Functional Theory (DFT), taking as reference the procedure implemented by Lin et al. (2006) in the Bi2212 compound. Results show that, the incorporation of Pb-dopant in Bi2223 lead a rigid displacement of the Bi/Pb–O bands toward higher energies, with a null contribution at the Fermi level, around the high symmetry point  $\bar{M}$  in the irreducible Brillouin zone, for Pb doping concentration equal to or more than 26%, avoiding the presence of the so-called Bi–O *pockets* in the Fermi surface, in good agreement with angle-resolved photoemission spectroscopy (ARPES) and nuclear magnetic resonance (NMR) experiments, although a slight metallic character of the Bi–O bonds is still observed which would disagree with some experimental reports. The calculations show that the changes on the structural properties are associated to the presence or absence of the Bi–O *pockets* in the Fermi surface.

© 2015 Elsevier B.V. All rights reserved.

## 1. Introduction

The  $\text{Bi}_2\text{Sr}_2\text{Ca}_2\text{Cu}_3\text{O}_{10}$  compound (Bi2223) is a high-temperature superconductor of the cuprate bismuth family with general formula  $\text{Bi}_2\text{Sr}_2\text{Ca}_{n-1}\text{Cu}_n\text{O}_{10}$ , which differ by the number of  $\text{CuO}_2$  planes per unit cell. Resistivity, susceptibility and magnetization experimental measurements in the Bi2223 compound ( $n = 3$ ) show a transition to the superconducting state at  $\sim 110$  K [1,2]. In spite of the fact that this compound has a very high viability for its use in industrial and technological applications [3–5], we found surprisingly a few theoretical reports.

In a previous work [6] we calculated the electronic properties of Bi2223 with tetragonal phase (I4/mmm), where the presence of electronic states associated with the Bi–O planes at the Fermi level ( $E_F$ ) was evident. These are observed in the Fermi surface (FS) as small closed surfaces around the anti-nodal point  $\bar{M}$  in the irreducible first Brillouin zone (IZB), in disagreement with experimental reports [7]. This issue is known as the Bi–O *pockets* problem [8,9] and has been present in the literature since long ago [10–15].

We have shown in a later work [16], that small changes in the position of the oxygen atom associated with the Sr plane in Bi2223, induce a quasi-rigid displacement of the Bi–O bands

towards higher energies avoiding its contribution at  $E_F$  offering a solution to the Bi *pockets* problem in theoretical calculations. It is necessary to validate experimentally these atomic positions.

Previously, Lin et al. showed that in the  $\text{Bi}_2\text{Sr}_2\text{Ca}_1\text{Cu}_1\text{O}_8$  compound (Bi2221) the Bi–O bands are lifted above  $E_F$  when Pb-dopant is incorporated in concentrations greater than 22%, avoiding the Bi–O *pockets* [8,9]. In that paper the authors state that this procedure has the same effect on the electronic properties of Bi2201 and Bi2223 compounds but without proof.

In this paper, we present a study of Pb doping effects on the structural and electronic properties of  $(\text{Bi}_{1-x}\text{Pb}_x)_2\text{Sr}_2\text{Ca}_2\text{Cu}_3\text{O}_{10}$  for  $0 \leq x \leq 0.35$ , using the ab initio virtual crystal approximation. We found that the Bi–O *pockets* disappear from the FS at a specific Pb doping, although a slight metallic character of the Bi–O bonds remains which would disagree with some experimental observations [17–19].

## 2. Method of calculation

The calculations were done using the full-potential linearized augmented plane wave method plus local orbital (FLAPW+lo) [20] within the local density approximation (LDA), using the wien2k code [21]. We used a plane-wave cutoff at  $R_{mt}K_{max} = 8.0$  and for the wave function expansion inside the atomic spheres, a maximum value for the angular momentum of  $l_{max} = 12$  with

\* Corresponding author. Tel.: +57 3108996440.

E-mail address: [jcamargo@unitropico.edu.co](mailto:jcamargo@unitropico.edu.co) (J.A. Camargo-Martínez).

**Table 1**

Optimized lattice parameters and atomic coordinates relaxed for  $(\text{Bi}_{1-x}\text{Pb}_x)_2\text{Sr}_2\text{Ca}_2\text{Cu}_3\text{O}_{10}$  with body-centered tetragonal structure and space group  $I4/mmm$ , for Pb concentrations of  $x = 0.0, 0.2, 0.25, 0.26, 0.3$  and  $0.35$ . The experimental values were taken from Ref. [23].

Parameter	Lattice parameters (Å)						
	Expt.	0.0	0.20	0.25	0.26	0.30	0.35
$a$	3.823(9)	3.8060	3.8058	3.8078	3.8080	3.8084	3.80787
$c$	37.074(5)	37.407	37.409	37.372	37.369	37.358	37.3692
$c/a$	9.6976(2)	9.8284	9.8294	9.8146	9.8134	9.8094	9.8137
Atomic coordinates							
Atom	Expt.	0.0	0.20	0.25	0.26	0.30	0.35
$\text{Bi}_{(1-x)}\text{Pb}_x$	0.2109(6)	0.2018	0.2034	0.2033	0.2035	0.2035	0.2031
Sr	0.3557(2)	0.3709	0.3693	0.3694	0.3685	0.3687	0.3689
Ca	0.4553(8)	0.4581	0.4576	0.4576	0.4572	0.4574	0.4575
Cu1	0.0000	0.0000	0.0000	0.0000	0.0000	0.0000	0.0000
Cu2	0.0976(4)	0.0823	0.0833	0.0832	0.0840	0.0837	0.0836
O1	0.0000	0.0000	0.0000	0.0000	0.0000	0.0000	0.0000
O2	0.0964(2)	0.0828	0.0834	0.0832	0.0835	0.0831	0.0830
O3	0.1454(4)	0.1477	0.1489	0.1488	0.1490	0.1486	0.1482
O4	0.2890(2)	0.2996	0.2992	0.2995	0.2992	0.2998	0.3002

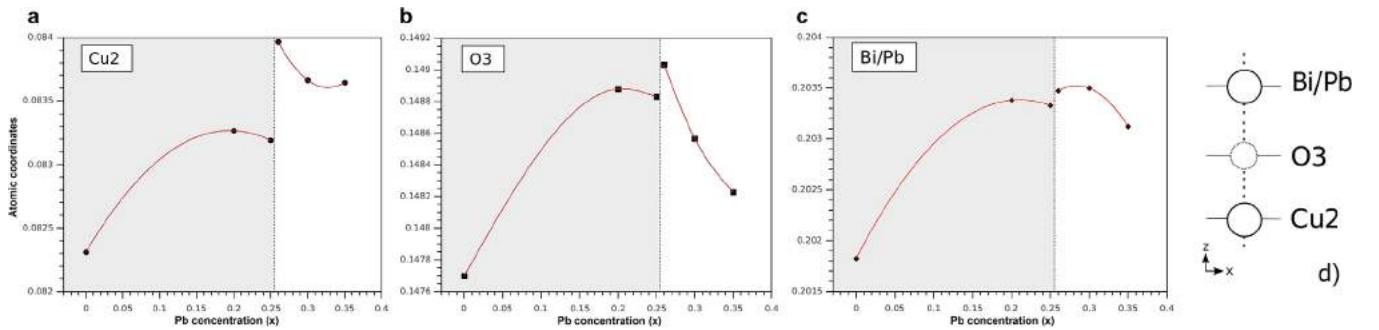


**Fig. 1.** Pb doping effects on the atomic coordinates of (a) Cu2, (b) O3 and (c) Bi/Pb in the  $\text{Bi}_2\text{Sr}_2\text{Ca}_2\text{Cu}_3\text{O}_{10}$  compound. (d) Schematic positions of Cu1, O3 and Bi/Pb in the structure.

$G_{max} = 20$ . We choose a  $14 \times 14 \times 14$   $k$ -space grid which contains 288 points within the IBZ. The muffin-tin sphere radii  $R_{mt}$  (in atomic units) were chosen to be 2.3 for Bi, 2.0 for Sr, 1.9 for both Ca and Cu, and 1.5 for O.

Pb substitution by Bi atoms was considered within the framework of the virtual crystal approximation (VCA), where the Bi nuclear charge  $Z$  is replaced by the average of the Bi and Pb charge of what may be thought as an “effective” Bi/Pb atom [8]. For this system it was found that the effective disorder parameter for the Bi–O states is  $\Delta/W \sim 0.33$ , where  $\Delta$  is the splitting of the Bi–O and Pb–O bands in Bi2223 and Pb2223, respectively and  $W$  the bandwidth, thus ensuring that the system is far from being in the split-band limit [8,9,22], confirming that the VCA is a good approximation in this case.

### 3. Results and discussion

#### 3.1. Structural properties

We studied the Pb doping effects on the structural properties of Bi2223 with a body-centered tetragonal structure (bct) and space group  $I4/mmm$  ( $D_{4h}^{17}$ ). The structure consists of three Cu–O planes, one Cu1–O1 plane between two Cu2–O2 planes, with Ca atoms between them. Each Cu2–O2 plane is followed by a Sr–O3 and Bi–O4 planes in that order.

Starting from the experimental parameters taken from Ref. [23], the  $c/a$  ratio was optimized by minimizing the total energy at a constant volume. Also the atomic coordinates were relaxed by minimizing the total force for each Pb concentration.

In Table 1 the values of the lattice parameters and the atomic coordinates obtained in this work are reported. In all cases, the

$c$  and  $a$  lattice parameters calculated show differences below 1% with respect to the reported experimental values. As a general behavior it is observed that the calculated values of  $c$  are always overestimated while those of  $a$  are underestimated as compared to the experimental data.

When the atomic coordinates are relaxed as a function of Pb concentration (see Table 1), a very sharp discontinuity in the value of the internal coordinates appears around  $x \sim 0.255$  dividing therefore the Pb doping effect on the structure into two distinct regions as it can be observed in Fig. 1 for the atoms Cu2, O3 and Bi/Pb.

It is found that the greater discontinuity occurs in the Cu2, which is interpreted as an important decrease in the internal parameter of Cu1 with Pb concentration (see Fig. 1a). O3 has a similar behavior, its proximity to Cu2 is enhanced for Pb concentrations greater than  $x = 0.25$ . The decrease in the Cu2–O3 distance has important effects on the electronic properties of Bi2223 [16]. In Fig. 1c, we show the effect that the introduction of Pb has on the atomic coordinates of the Bi/Pb in Bi2223. Notice the discontinuity at  $x = 0.255$ . It is not as strong as the one in Cu2 and O3. It is observed a steadily increase of the internal parameter which is almost quadratic and presents a maximum Pb-concentration at approximately  $x = 0.28$ .

We show in Fig. 2 the effects of Pb doping on the Cu2–O3 and Bi/Pb–O3 relative distances ( $d_{\text{Cu2-O3}}/c$  and  $d_{\text{Bi/Pb-O3}}/c$ , respectively). Initially, doping induces a progressive increase of the Cu2–O3 distance (see Fig. 2a). This behavior changes completely for Pb concentrations greater than 0.25. For a Pb concentration of 0.26, i.e., Pb doping of 26%, the Cu2–O3 distance is 2.43 Å, which is 0.6–0.8 Å greater than the experimental values reported [23–27]. The difference with experiment is clear. In Fig. 2b, we show the

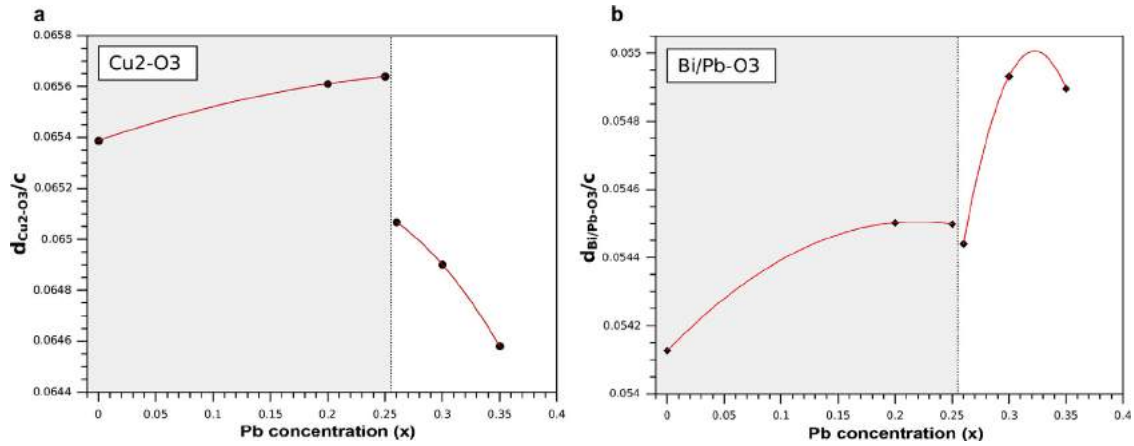


Fig. 2. Pb doping effects on the (a) Cu2-O3 and (b) Bi/Pb-O3 relative distances ( $d_{\text{Cu}2-\text{O}3}/c$  and  $d_{\text{Bi/Pb}-\text{O}3}/c$ , respectively) in the  $\text{Bi}_2\text{Sr}_2\text{Ca}_2\text{Cu}_3\text{O}_{10}$  compound.

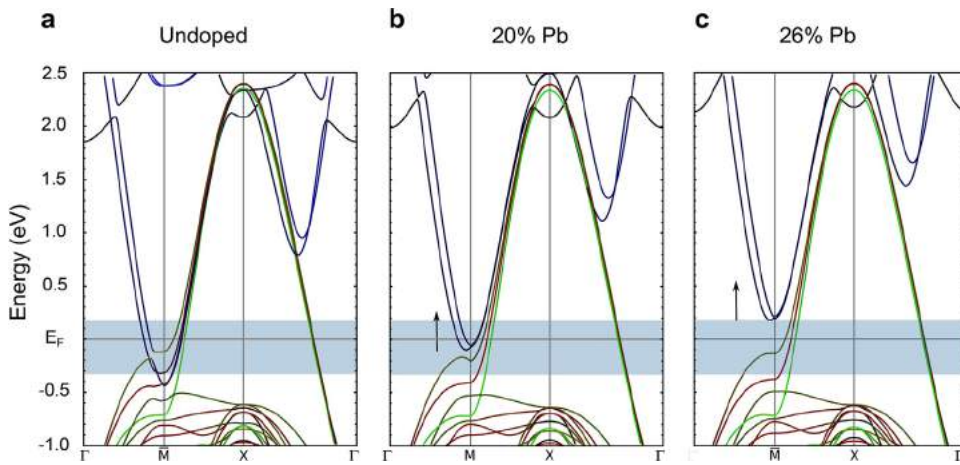


Fig. 3. Pb doping effects on the band structure of the  $\text{Bi}_2\text{Sr}_2\text{Ca}_2\text{Cu}_3\text{O}_{10}$  compound for the Pb concentration of (a) 0.0 (Undoped), (b) 0.2 (20% Pb) and (c) 0.26 (26% Pb). The blue, red and green lines represent the Bi  $p$ , Cu2  $d$  and Cu1  $d$  states, respectively. The hybridized states from these bands are represented by their respective color mixture and the black line represents the other states. (For interpretation of the references to color in this figure legend, the reader is referred to the web version of this article.)

$d_{\text{Bi/Pb}-\text{O}3}/c$  as a function of Pb-doping. It has a maximum at  $x = 0.26$ . The discontinuity between 0.25 and 0.26 is not as big as the  $d_{\text{Cu}2-\text{O}3}/c$ . Nevertheless an important change is observed between the concentrations 0.26 and 0.3.

In Figs. 1 and 2 two regions are distinguished, the gray region represents the presence of Bi-O *pockets* in the FS and the white area indicates the absence of them. In these regions the behavior of the structural properties clearly shows notable differences associated to the presence (or absence) of the Bi-O *pockets*.

### 3.2. Electronic properties

The electronic properties of Pb-free and Pb-doped Bi2223 are different in three regions. In the first, Pb-free Bi2223 shows the presence of Bi-O *pockets* in the FS due to the interaction between Cu-O and Bi-O4 planes by the mediation of O3, in total disagreement with the experimental reports [7]. In the second, the Pb substitution (20–25%) on the Bi sites in Bi2223 produces a significant reduction in the interaction between Cu-O and Bi-O4 planes but still the contribution of the Bi-O states at  $E_F$  around point  $\bar{M}$  remains. The third one, containing 26% Pb or more, shows an almost null interaction between the Cu-O and Bi-O4 planes and, consequently, the contribution of the Bi-O states at  $E_F$  is minimal and the Bi-O *pockets* are not observed in the FS. The band structures of Pb-free and Pb-doped Bi2223 with Pb concentration of  $x = 0.0$  (Undoped), 0.25 (25% Pb) and 0.26 (26% Pb) are shown in Fig. 3.

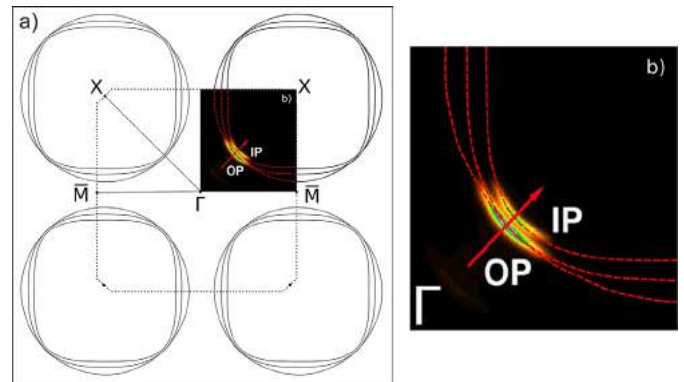


Fig. 4. (a) The Fermi Surface (FS) at  $k_2 = 0$  of  $\text{Bi}_2\text{Sr}_2\text{Ca}_2\text{Cu}_3\text{O}_{10}$  compound in an extended zone scheme, for Pb concentration of 26% ( $x = 0.26$ ). (b) The experimental FS reported by Ideta et al. measured in the nodal direction by angle-resolved photoemission spectroscopy (ARPES) [7], compared with our results (red dashed line). (For interpretation of the references to color in this figure legend, the reader is referred to the web version of this article.)

For Pb-free Bi2223, see Fig. 3a, partially filled Bi-O bands around the anti-nodal point  $\bar{M}$  were observed which hybridize with the Cu-O bands. Notice the metallic character of the Bi-O plane and the presence of Bi-O *pockets* in the FS, in disagreement with experimental reports [7]. A detailed analysis of this band

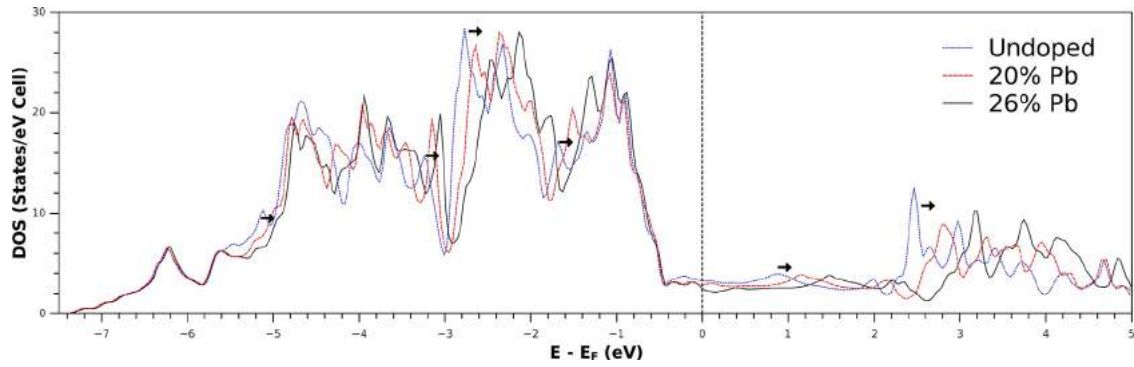


Fig. 5. Pb doping effects on the total density of states (DOS) in the  $\text{Bi}_2\text{Sr}_2\text{Ca}_2\text{Cu}_3\text{O}_{10}$  compound, for Pb concentrations of (a) 0.0 (undoped), (b) 0.2 (20% Pb) and (c) 0.26 (26% Pb).

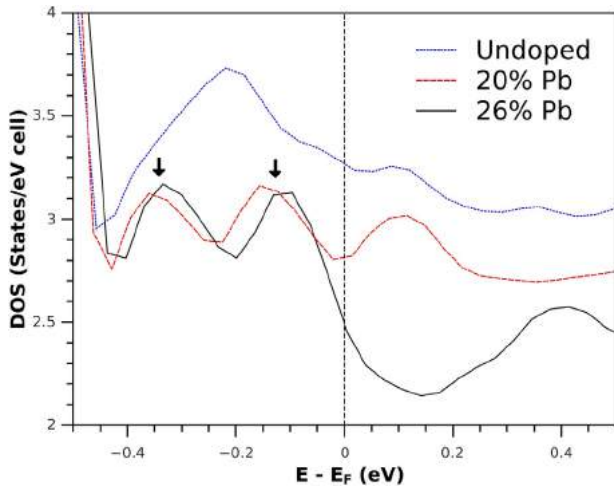


Fig. 6. Pb doping effects on the total density of states (DOS) around  $E_F$  in the  $\text{Bi}_2\text{Sr}_2\text{Ca}_2\text{Cu}_3\text{O}_{10}$  compound, for Pb concentrations of (a) 0.0 (undoped), (b) 0.2 (20% Pb) and (c) 0.26 (26% Pb). Arrows indicate two peaks at binding energies of  $-0.35$  and  $-0.15$  which are associated with the extended van Hove singularities.

structure can be found in Ref. [6]. Fig. 3b shows the band structure of Bi2223 when the 20% of Bi is replaced by Pb ( $x = 0.20$ ). A rigid displacement of the Bi/Pb–O bands toward higher energies is observed. These bands are partially filled and contribute at  $E_F$ . The hybridization with the Cu–O bands is apparently null. The extended van Hove singularities (VHSs) appear at binding energies of  $-0.35$  and  $-0.15$  eV.

When Pb concentration is equal to or greater than 26% ( $x = 0.26$ ), see Fig. 3c, the empty Bi/Pb–O bands are lifted rigidly above  $E_F$  with no contribution at  $E_F$  around the point  $\bar{M}$  avoiding apparently the Bi–O pockets problem. The Cu–O bands do not suffer any significant effect due to Pb doping keeping the reported characteristic behavior of cuprates. An identical result (Fig. 3c) was reported in a previous paper [16] where without Pb doping with a simple displacement of the O3 atom instead towards the Bi one (away from Cu2), the same movement of the Bi–O bands was induced avoiding completely its contribution at  $E_F$ . This atomic displacement avoided the charge transfer between Cu2 and Bi through O3, eliminating the metallic character of Bi–O4 plane. As mentioned before, the presence of the Bi–O pockets are associated to the interaction between Cu–O and Bi–O planes. The presence of Pb in Bi2223 using the VCA, can be interpreted as a reduction of electric charge in the Bi that avoids the presence of possible electronic states that participate in Cu2–O3–Bi interaction, which filled the Bi–O band.

Fig. 4 shows the calculated FS for Pb-doped Bi2223 at 26% compared to the experimental FS reported by Ideta et al. which was measured in the nodal direction by angle-resolved photoemission spectroscopy (ARPES) [7]. This experiment revealed the presence of two surfaces which were assigned to the outer copper Cu2–O2 planes (OP) and to the inner copper Cu1–O1 plane (IP).

The calculated FS (see Fig. 4a) shows three concentric closed surfaces around point X of the IBZ, without the presence of so-called Bi–O pockets around the  $\bar{M}$  point. Two of this surfaces show quasi-degeneration in the nodal direction which are associated with Cu2–O2 (OP) planes, while the other surface come from the Cu1–O1 plane (IP). These results show a very good agreement with

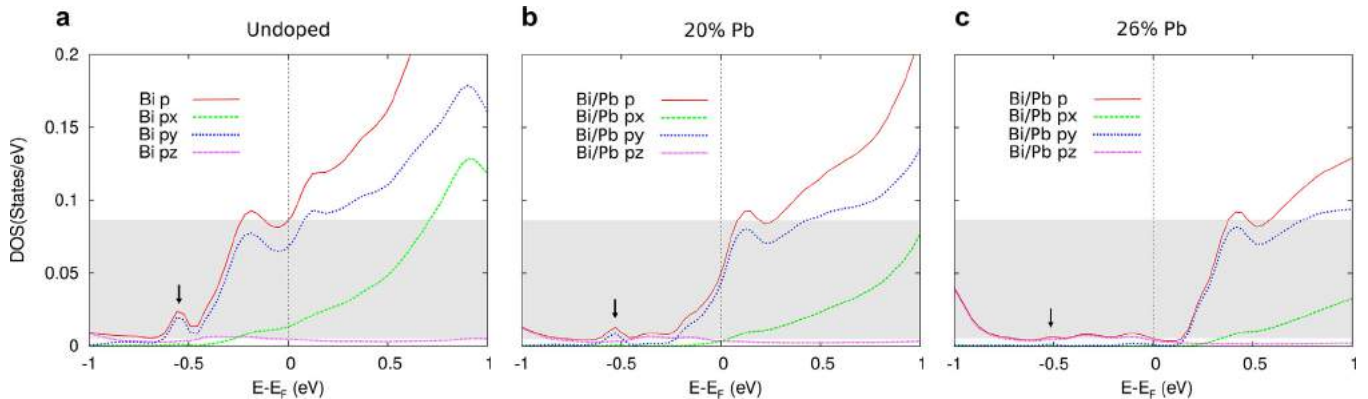
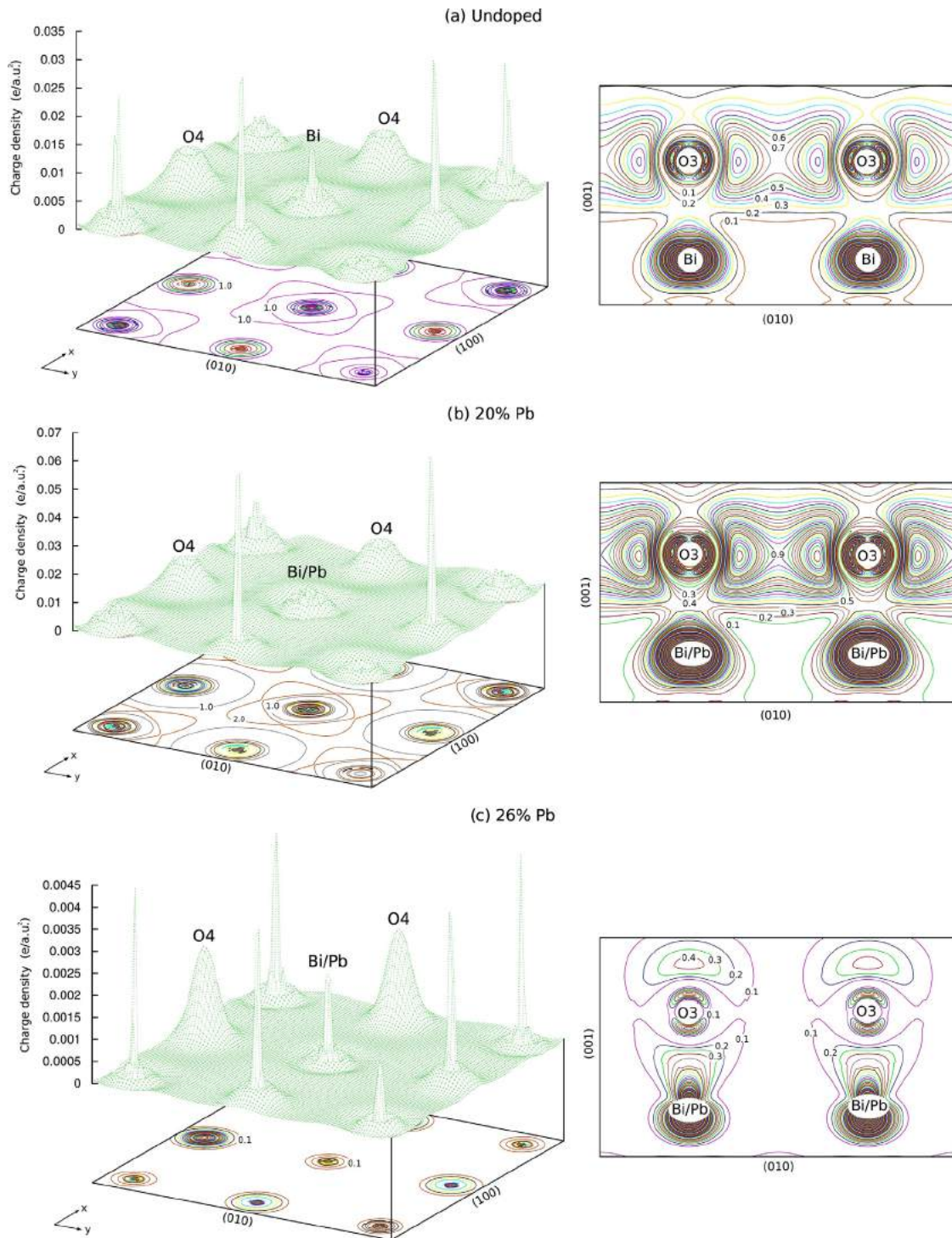


Fig. 7. Pb doping effects on the total density of states (DOS) of the Bi  $p$  around  $E_F$  in the  $\text{Bi}_2\text{Sr}_2\text{Ca}_2\text{Cu}_3\text{O}_{10}$  compound, for Pb concentrations of (a) 0.0 (undoped), (b) 0.2 (20% Pb) and (c) 0.26 (26% Pb). Arrow indicates one peak at energy of  $-0.49$  eV.



**Fig. 8.** 2D and 3D charge density calculations around  $E_F$  in the Bi-O plane of the Pb-doped Bi2223 compound, for Pb concentrations of (a) 0.0 (undoped), (b) 0.2 (20% Pb) and (c) 0.26 (26% Pb), obtained with XCrySDen program [31]. Scale units of e/a.u.<sup>2</sup>.

experiment [7] (see Fig. 4), as well as with studies of nuclear magnetic resonance (NMR) where it was reported that the hole concentration of OP is larger than IP [28,29].

The Pb doping effects on the total density of states (DOS) in Bi2223 are presented in Fig. 5. These DOS show that  $E_F$  falls in a region of low DOS, a typical behavior of these Cu-O based superconductors. As a general behavior, Pb doping induces a displacement towards higher energies in the DOS, which leads to changes in the contribution of the electronic states at  $E_F$ .

Fig. 6 shows that the DOS at  $E_F$ ,  $N(E_F)$ , decreases as Pb doping increases in Bi2223. The extended van Hove singularities (VHSs) appear at binding energies of  $-0.35$  and  $-0.15$  eV, respectively, which play an important role in the physics of high-temperature superconductors [30].

$N(E_F)$  in the Pb-free Bi2223 is 3.27 states/(eV cell) which has contributions from Cu-O and Bi-O planes, mainly of Cu  $d_{x^2-y^2}$ -O  $p_x, y$  and Bi  $p_x, y$ -O3  $p_x, y$ -O4  $p_x, y$  states, showing the metallic character of Bi-O plane. The contribution of the Bi-O states at  $E_F$  (Bi-O

pockets) is due to the interaction between Cu–O and Bi–O planes, as shown in the hybridization of their respective energy bands, see Fig. 3a. This  $N(E_F)$  also has a small contribution of Cu  $d_{z^2}$ –O  $p_z$  and Bi  $p_{z-03}$   $p_{z-04}$   $p_z$  states.

At 20% Pb, the contribution of the Cu–O and Bi–O planes at  $E_F$  decreases to 7% and 56% respectively, i.e., the interaction between Cu–O and Bi–O states decreases significantly. The Bi  $p_{x,y-03}$   $p_{x,y-04}$   $p_{x,y}$  states are the ones that decrease the most their contribution at  $E_F$  which becomes 2.81 states/(eV cell) meanwhile Bi  $p_{z-03}$   $p_{z-04}$   $p_z$  states are not affected by the presence of Pb in the structure. With increasing Pb doping up to 25% the electronic properties show no significant changes.

Further,  $N(E_F)$  is 2.49 states/(eV cell) when Pb doping is 26%; the contribution at  $E_F$  of Bi  $p_{x,y-03}$   $p_{x,y-04}$   $p_{x,y}$  states is almost null, although a contribution of Bi  $p_{z-03}$   $p_{z-04}$   $p_z$  states is observed, representing a little more than 1% of the total contribution at  $E_F$ , which can be interpreted as a slight metallic character of Bi–O plane. For 26% Pb doping, this metallic character is maintained. The presence of these Bi–O states comes from the energy bands that intersect at  $E_F$  in the  $\bar{M}$ –X direction, see Fig. 3c.

Fig. 7 shows the influence of Pb doping on the DOS of the Bi  $p$  at the Fermi level for different concentrations 0.0, (Undoped), 0.2 (20% Pb) and 0.26 (26%). As in the electronic band structure, an almost rigid displacement toward higher energies is observed as the Pb concentration changes. As a consequence, the number of states at the Fermi level diminishes. This is mainly due to the behavior of Bi  $p_x$  and Bi  $p_{xy}$ . In Fig. 7, the zone in grey represents the change of the mentioned contribution at  $E_F$ . In Fig. 7a and b a maximum at  $-0.49$  eV of states Bi  $p_y$  (arrow) is associated with the interaction between the Cu and Bi planes. This maximum does not show any displacement towards higher energies but instead towards lower energies as the Pb content diminishes in Bi2223 and even disappears for concentrations equal or higher than 0.26 (26%) when the contribution of the Cu and Bi planes is zero (no BiO pockets). Finally, at  $E_F$  a small contribution of Bi/Pb  $p_z$  states.

In Fig. 8, the effect of Pb content on the charge density in the Bi/Pb–O4 plane and on the Bi/Pb–O3 bond for concentrations 0.0 (undoped), 0.2 (20%) and 0.26 (26%) is shown.

For 0.0 (undoped) and 20% concentration, Fig. 8a and b, the charge density on the Bi/Pb–O4 and on the Bi/Pb–O3 bond are similar. On the Bi/Pb–O3 crystalline bond, the bonding character of O3  $p_{y(x)}$ –O3  $p_{y(x)}$  is observed as well as the character anti-bonding of the Bi/Pb  $p_{y-03}$   $p_{y(x)}$  which persist even when the BiO pockets are present. For 0.26 (26%) concentration (Fig. 8c) important changes occur in the charge density on the Bi/Pb–O4 plane and on the Bi/Pb–O3 bond with respect to the concentrations 0.0 (undoped) and 0.2 (20%). On the Bi/Pb–O3 bond, the anti-bonding character Bi/Pb  $p_{z-03}$   $p_z$  is observed. This holds even after the displacement of the Bi–O bands to energies higher than  $E_F$ . The Bi/Pb–O4 plane has a smaller charge density due to the lower contribution of Bi states at  $E_F$  and to the absence of the BiO pockets.

Experimental results using scanning tunneling microscopy (STM) show that the Bi–O planes are non-metallic in Bi2212 [17–19]. To the best of our knowledge there are no experiments that define the metallic or non-metallic character of the Bi–O planes in Bi-2223, except for the report presented by Asokan et al. that using X-ray absorption near edge structure (XANES), show a metallic character of Bi–O planes for Bi-2223 and Bi-2212 [32]. The last one is in disagreement with the previous works just mentioned.

We reproduce the calculations reported by Lin et al. [9] and effectively it was found that for Pb doping concentration equal to or more than 22% the Bi–O bands move toward higher energies avoiding its contribution at  $E_F$  on the point  $\bar{M}$  (no Bi–O pockets in FS).

Although it was also found in this case that, as in Bi2223, a slightly metallic character in the Bi–O bonds due to contribution of Bi–O states at  $E_F$  on  $\bar{M}$ –X direction is observed, in disagreement with some the Bi2212 experimental reports. Thus, Pb doping in Bi2212 and Bi2223 structures certainly avoids the presence of the pockets at FS, although the metallic character of the Bi–O planes remains. In conclusion, the nature of Bi–O planes for Bi-2223 needs to be tested with more experiments.

#### 4. Conclusions

In this paper, we presented a study of Pb doping effects on the structural and electronic properties of  $(\text{Bi}_{1-x}\text{Pb}_x)_2\text{Sr}_2\text{Ca}_2\text{Cu}_3\text{O}_{10}$  for  $0 \leq x \leq 0.35$ , using the Local Density (LDA) and Virtual Crystal (VCA) approximations within the framework of the Density Functional Theory (DFT) with the Wien2k code. We have followed the method applied in Bi2212 by Lin et al. [8,9] to study of Bi2223.

Our results show significant changes in Bi2223 structural properties when Pb is incorporated as a dopant. These changes are associated to the presence or absence of the Bi–O pockets at the Fermi surface (FS). The most relevant feature is observed in Cu2–O3 distance, which becomes lower when the Bi–O pockets disappear from the FS. Although differences between experimental parameters,  $a$  and  $c$ , and the calculated ones are not greater than 1%, appreciable discrepancies in the interatomic distances are observed, as in the case of the Cu2–O3 distance which is 0.6–0.8 Å greater than the experimental values reported.

It was observed, as a general feature that Pb doping in Bi2223 leads to a rigid displacement of the Bi/Pb–O bands toward higher energies with a null contribution at the Fermi level in the high symmetry point  $\bar{M}$  of IBZ for Pb doping concentrations equal to or more than 26%. This displacement, avoids the presence of the so-called Bi–O pockets at the FS, in good agreement with angle-resolved photoemission spectroscopy (ARPES) and nuclear magnetic resonance (NMR) experiments. A slightly metallic character of the Bi–O planes still remains due to the contribution of the Bi  $p_{z-03}$   $p_{z-04}$   $p_z$  states at  $E_F$  in the  $\bar{M}$ –X direction. The Cu–O bands do not suffer any significant effect due to Pb doping, keeping the reported characteristic behavior of the cuprates.

The metallic character of the Bi–O bonds is also observed in Bi2212. this result disagrees with some experimental reports. Thus, the absence of the Bi–O pockets does not guarantee the non-metallic character of the Bi–O planes in either Bi2212 or Bi2223 compounds.

We have found following Refs. [8,9] that the Bi–O pockets disappears the FS at 26% Pb doping (and above) for Bi2223.

#### Acknowledgments

The authors acknowledge to the Fundación Universitaria Internacional del Trópico Americano under the Project 2014BINV0004, for providing resources that contributed to the research results reported within this paper.

#### References

- [1] J.L. Tallon, R.G. Buckley, P.W. Gilberd, M.R. Presland, I.W.M. Brown, M.E. Bowden, L.A. Chistian, R. Goguel, Nature 333 (1988) 153.
- [2] J.M. Tarascon, W.R. McKinnon, P. Barboux, D.M. Hwang, B.G. Bagley, L.H. Greene, G.W. Hull, Y. LePage, N. Stoffel, M. Giroud, Phys. Rev. B 38 (1988) 8885.
- [3] H. Kitaguchi, H. Kumakura, Advances in Bi-based high- $T_c$  superconducting tapes and wires, MRS Bull. 26 (2001) 12.

- [4] T.J. Arndt, A. Aubele, H. Krauth, M. Munz, B. Sailer, A. Szulczyk, IEEE Trans. Appl. Supercond. 13 (2003) 3030.
- [5] W. Hassenzahl, et al., Electric power applications of superconductivity, Proc. IEEE. Special Issue on Applications of Superconductivity 92 (10) (2004) 1655.
- [6] J.A. Camargo-Martínez, D. Espitia, R. Baquero, Rev. Mex. Fis. 60 (1) (2014) 39.
- [7] S. Ideta, et al., Phys. Rev. Lett. 104 (2010) 227001.
- [8] H. Lin, et al., Phys. Rev. Lett. 96 (2006) 097001.
- [9] H. Lin, Topics in Electronic Structure and Spectroscopy of Cuprates, Northeastern University, 2008 Ph.d. thesis.
- [10] S. Massidda, J. Yu, A.J. Freeman, Phys. C 152 (1988) 251.
- [11] H. Krakauer, W.E. Pickett, Phys. Rev. Lett. 60 (1988) 1665.
- [12] D.J. Singh, W.E. Pickett, Phys. Rev. B 51 (1995) 3128.
- [13] A. Damascelli, et al., Rev. Mod. Phys. 75 (2003) 473.
- [14] H. Matsui, et al., Phys. Rev. B 67 (2003) 060501.
- [15] D.L. Feng, et al., Phys. Rev. Lett. 88 (2002) 107001.
- [16] J.A. Camargo-Martínez, D. Espitia, R. Baquero, Rev. Mex. Fis. 61 (2) (2015) 88.
- [17] M. Tanaka, et al., Nature 339 (1989) 691.
- [18] S.M. Butorin, et al., Phys. Rev. B 51 (1995) 11915.
- [19] B.O. Wells, Z.-X. Shen, D.S. Dessau, W.E. Spicer, C.G. Olson, D.B. Mitzi, A. Kapitulnik, R.S. List, A. Arko, Phys. Rev. Lett. 65 (1990) 3056.
- [20] O.K. Andersen, Phys. Rev. B 12 (1975) 3060.
- [21] P. Blaha, K. Schwars, G.K.H. Madsen, D. Kvasnicka, J. Luitz, in: K. Schwars (Ed.), WIEN2K, An Augmented Plane Wave + Local Orbitals Program for Calculating Crystal Properties, Vienna University of Technology, Austria, 2001.
- [22] A. Bansil, Phys. Rev. B. 20 (1979) 4035.
- [23] X. Zhu, S. Feng, J. Zhang, G. Lu, K. Chen, K. Wu, Z. Gan, Mod. Phys. Lett. B 3 (1989) 707.
- [24] Y. Ji-Lian, et al., Mod. Phys. Lett. B 4 (1990) 791.
- [25] T. Kozuka, H. Ogawa, A. Kan, A. Suzumura, J. Eur. Ceram. Soc. 21 (2001) 1913.
- [26] N. Kijim, H. Endo, J. Tsuchita, M. Mizuno, Y. Oguri, Jpn. J. Appl. Phys. 28 (1989) L787.
- [27] V.F. Shamray, A.B. Mikhailova, A.V. Mitin, Cryst. Rep. 54 (2009) 584.
- [28] A. Trokiner, Phys. Rev. B 44 (1991) 2426.
- [29] H. Kotegawa, et al., J. Phys. Chem. Solids 62 (2001) 171.
- [30] R.S. Markiewicz, Phys. C 127 (1993) 381.
- [31] A. Kokalj, Comp. Mater. Sci. 28 (2003) 155.
- [32] K. Asokan, et al., J. Electron Spectrosc. 114 (2001) 837.